

Ultrafast Nonlinear Photoresponse of Single-Wall Carbon Nanotubes: A Broadband Degenerate Investigation

Shuo Xu,¹ Fengqiu Wang,^{1,*} Chunhui Zhu,¹ Yafei Meng,¹ Yujie Liu,¹ Wenqing Liu,¹ Jingyi Tang,² Kaihui Liu,^{2,*} Guohua Hu,³ Richard Howe,³ Tawfique Hasan,³ Rong Zhang,¹ Yi Shi,¹ and Yongbing Xu^{1,*}

¹ School of Electronic Science and Engineering and Collaborative Innovation Center of Advanced Microstructures, Nanjing University, Nanjing 210093, China

² State Key Laboratory for Mesoscopic Physics, School of Physics and Collaborative Innovation Center of Quantum Matter, Peking University, Beijing 100871, China

³ Cambridge Graphene Centre, University of Cambridge, Cambridge CB3 0FA, UK

*Authors to whom correspondence should be addressed. Electronic addresses: wang@nju.edu.cn, khliu@pku.edu.cn, and ybxu@nju.edu.cn

Abstract: Understanding of the fundamental photoresponse of carbon nanotubes has broad implications for various photonic devices. Here, Z-scan and pump-probe spectroscopy were combined to map the ultrafast nonlinear optical properties of single-wall carbon nanotubes (SWNTs), spanning 600-2400 nm. In contrast to conventional view, sizable saturable absorption is observed across the visible to the near-infrared range, including regions between semiconducting excitonic peaks and metallic tube transitions. Further, a cut-off for saturable absorption, attributed to photoinduced broadening of the transition linewidth, is identified within the first semiconducting excitonic band at ~2100 nm. Our findings provide answers to existing controversies over SWNTs' broadband nonlinear absorption characteristics, and suggest that photoinduced effects may play an active role in determining the ultrafast nonlinear photoresponse of SWNT ensembles.

Single-wall carbon nanotubes (SWNTs), a model one-dimensional quantum confined system with fascinating physics,^{1,2,3} have been widely explored for optical and optoelectronic applications.^{4,5,6} In particular, broad absorption range combined with an ultrafast relaxation time has raised a great deal of interests in using SWNTs as a nonlinear optical materials.^{3,7,8} It is desirable to obtain quantitative information about optical transitions in SWNTs over an extended spectral range, as it provides important insights into light-matter interactions in such low-dimensional systems. To this end, photoexcitation of SWNTs in the linear regime has been extensively studied and well interpreted.^{9,10} On the other hand, the nonlinear photoexcitation in SWNTs, which is governed by photocarrier processes following high-intensity ultra-short pulse irradiation, is equally important.^{11,12,13,14,15,16} Understanding of the photophysics in such excitation regimes may directly impact functionalities in various photonic devices.

One application involving nonlinear photoexcitation of SWNTs, that has drawn widespread attention, is the generation of ultrashort pulses in solid-state or fiber lasers through a technique known as mode-locking, where a bleached absorption (or saturable absorption) in SWNTs together with an ultrafast photocarrier relaxation provides a mechanism for short pulse formation and stabilization.^{17,20} Although a large number of mode-locked lasers based on SWNT saturable absorbers have been reported since 2003,^{18,19,20,21,22} several open questions still remain. For example, while it is conventionally believed that saturable absorption is provided by resonantly excited semiconducting nanotubes (due to Pauli blocking effect), more recent experiments have suggested that operations at wavelengths far off these resonant bands are possible.^{23,24} Another question concerns the cut-off wavelengths for saturable absorption.²⁵ For example, whether SWNTs could operate beyond their semiconducting excitonic bands into the mid-infrared is still unclear. Probing the broadband characteristics of key ultrafast nonlinear optical properties of SWNTs, including saturable absorption (or equivalently, modulation depth) and relaxation time constant, may provide crucial experimental evidence for answering these still elusive questions. Pump-probe spectroscopy using widely tunable probe energies, i.e. provided by supercontinuum sources, have been carried out to map different photobleaching (PB) and photoinduced absorption (PA) bands, but these are usually non-degenerate (two-color) measurements, which involve excited states and carrier relaxation pathways that are appreciably different from the two-level model depicting behavior of SWNT saturable absorbers.^{14,15,16} Therefore the results cannot be directly applied to the interpretation of SWNT saturable absorber response. Z-scan or degenerate pump-probe techniques, using single excitation wavelength, are directly relevant to resolving saturable absorption dynamics and have been reported in several

studies.^{3, 8, 26} However, most of the previous investigations were carried out at discrete wavelengths, and on SWNT samples of different morphological forms. Thus, it is challenging to correlate the results, making it difficult to gain broadband quantitative insights into the signatures of nonlinear photoresponse in SWNTs.

This work, to the best of our knowledge, is the first attempt to establish a broadband mapping of key ultrafast nonlinear absorption properties of SWNTs. To this end, we have combined Z-scan and degenerate pump-probe measurements on the same SWNT sample across 600-2400 nm, covering multiple excitonic bands. The knowledge of the photoexcitations in the SWNT ensembles based on a phenomenological model allows us to assign the observed spectral signatures to different transitions of the constituent tubes. In contrast to the conventional view, we have identified sizable saturable absorption in the spectral region between S₁₁ and S₂₂ excitonic peaks (~1200-1600 nm), as well as the metallic M₁₁ excitonic band (~600-800 nm), suggesting that SWNTs may exhibit broadband saturable absorption extending from visible to the near infrared range. Importantly, a transition from PB to PA in the pump-probe spectroscopy is identified within the semiconducting S₁₁ band (~2100 nm), signifying increasing tendency of reverse saturable absorption operation towards longer wavelengths. Such a feature, attributable to photoinduced linewidth broadening, underpins the importance of considering multiple physical effects in engineering the spectral response of SWNTs. The nonlinear photoexcitation signatures reported here help resolve the elusive questions regarding SWNT saturable absorbers and provide updated design guidelines for nanotube based nonlinear optical devices.

Results and discussions

To ensure intrinsic optical response from SWNTs, we used commercially available purified arc-discharge SWNTs that are surfactant free (Carbon Solutions Inc). SWNT-carboxymethyl cellulose composite film with ~50 μm thickness are fabricated using a solution processing method described in Ref. 22. No aggregates or large bundles are present in the film. Figure 1 shows the measured optical absorption of the SWNT sample. A tube diameter distribution of ~1.3-1.6 nm can be inferred from the absorption peak positions¹⁰ as well as Raman measurements (See Fig.S1).^{6, 27} The three absorption features correspond to the S₁₁ semiconducting excitonic band ~ 1800 nm, the S₂₂ semiconducting excitonic band ~ 1000 nm, and the M₁₁ metallic excitonic band ~ 700 nm, respectively.²⁸ Dashed lines in Fig.1 denote the

calculated absorption spectra for nanotube ensembles with 1.3-1.6 nm diameters, based on a phenomenological model for suspended individual nanotube.⁹ It provides a qualitative reference for the contribution to photoexcitation from different constituent tubes (Supplementary Note).

As nonlinear absorption characteristics of SWNTs is our focus, an open-aperture Z-scan setup is employed. The pump source consists of a 1 kHz Ti : Sapphire amplifier system with an optical parametric amplifier (OPA). The excitation pulse duration is ~100 fs. Such a system is good for delivering high peak intensities while reducing thermal effects. For the Z-scan measurement, we are confined to a wavelength range of 600-1800 nm, as limited by the power meter sensors. However, this already covers all the main excitonic features of the SWNT sample. To better interpret the broadband Z-scan results and to extend the spectral coverage of the mapping further into the mid-infrared, we used a degenerate pump-probe spectroscopy setup with parallel polarization configurations where the wavelength can be tuned within 1200-2400 nm. Thus, for the spectral overlap region, i.e. 1200-1800 nm, pump-probe data is used to corroborate with the Z-scan results.

We first look at the nonlinear optical response at on-resonance wavelengths. At each excitation wavelength, to avoid laser damage caused by either high peak intensities or thermal effects, we have limited our excitation power to a range within which Z-scan curves are readily reproducible without change in its nonlinear optical response. Figure 2 shows the open-aperture Z-scan results for 1800 nm (S_{11}), 1000 nm (S_{22}), and 700 nm (M_{11}), respectively. At relatively low incident powers, the sample exhibits saturable absorption behavior, while reverse saturable absorption generally attributed to two-photon absorption can be observed at elevated power levels³². To analyze the characteristics of saturable absorption, peak intensities of the incident beam is calculated for each sample position z using equation (1), where I_0 is the incident peak intensity, $z_0 = \pi \omega_0^2 / \lambda$ is the diffraction length of the beam, E is the incident pulse energy, ω_0 is the beam waist radius, and τ is the full width at half maximum of the excitation pulses:

$$I(z) = \frac{I_0}{1 + z^2/z_0^2}, I_0 \approx \frac{E}{\pi \omega_0^2 \cdot \tau} \quad (1)$$

We evaluate the saturable absorption α_0 , the modulation depth $\Delta = \alpha_0 / (\alpha_0 + \alpha_{ns})$ and the saturation intensity I_{sat} using a classic saturable absorber model, where α and α_{ns} denote linear and non-saturable absorption respectively.²⁹

$$\alpha(I) = \frac{\alpha_0}{1 + I/I_{sat}} + \alpha_{ns} \quad (2)$$

This results in the nonlinear absorption curves as shown in Fig.3, where pronounced saturable absorption can be seen for all resonant wavelengths. The inset of Fig.3 displays the nonlinear absorption as a function of the excitation intensity on a linear scale. This clearly illustrates the differences in modulation depths at different resonances. The strongest saturable absorption is observed for the S₁₁ and S₂₂ resonances, where a modulation depth of ~59% and ~41% are achieved, respectively. What is worth noting is the observation of a sizable saturable absorption, i.e. ~20%, for the M₁₁ resonant wavelength. Since metallic tube transitions dominate at this wavelength, as seen from the calculated absorption spectra in Fig.1, our observation suggests that SWNTs may exhibit saturable absorption in the visible range, although the saturation intensity is somewhat higher than the semiconducting resonances, probably due to the faster relaxation time typically observed in metallic tubes.¹¹

We then performed open-aperture Z-scan at a range of other wavelengths from 600 nm to 1800 nm. This allows the resonance-dependent saturable absorption, modulation depth and saturation intensity to be revealed, as shown in Figure 4. Note that an additional data point for 1950 nm is obtained from a thulium fiber laser-based nonlinear absorption measurement (See Fig.S3). Clearly, the modulation depth for resonant wavelengths within the S₁₁, S₂₂ bands is enhanced, as expected from previous studies.¹⁸ However, more informative findings are obtained outside of the S₁₁, S₂₂ bands. First, we detect appreciable modulation depth (~ 7-20%) between 600 nm and 800 nm, a range where transitions in metallic tubes are the main contributors to photoexcitation. Such a response suggests that SWNTs may act as an effective saturable absorber for the UV-visible range, i.e. suitable for mode-locking visible-emitting diodes or fluoride fiber lasers. On the other hand, for the spectral region in between S₁₁ and S₂₂ peaks, i.e. 1200-1600 nm, a flat but still sizable saturable absorption response is observed. This is in contrast to the results obtained by transient absorption spectroscopy, where a photoinduced absorption band is found to occupy the nonresonant region between S₁₁ and S₂₂ peaks.¹⁴ While the exact origin for photoexcitation in this spectral range is still unclear,^{15,30} our Z-scan results nevertheless highlight the importance of using single-color excitation for characterizing saturable absorption behavior. It is noted that although the modulation depth stays relatively constant from 1200-1600 nm, an increase in I_{sat} , from 200 MW/cm² to ~ 600 MW/cm², is observed as the excitation

wavelength is tuned from 1600 nm to 1200 nm (Fig.4b). For the semiconducting resonant bands, I_{sat} is found to be lower, within the range of $\sim 50\text{-}300 \text{ MW/cm}^2$, which is in agreement with previous characterizations.³¹

To gain full physical picture of the nonlinear photoresponse of the SWNTs, particularly towards the long wavelength end, we complement our Z-scan results with a single-color pump-probe experiment performed between 1200 and 2400 nm. Figure 5(a) shows the transient absorption curves at a pump fluence of $\sim 0.3 \text{ mJ/cm}^2$ for selected wavelengths between 1200-2400 nm (where probe fluence is at least 20 fold lower than the pump). The experimental measurements can be well fitted by a single exponential decay.³⁰ Several features were revealed by corroborating with the Z-scan measurements. First, we extract the peak value of $\Delta T/T_0$ from the pump-probe curves, as shown in Fig. 5(b). Similar to the modulation depth spectra obtained by Z-scan, the peak $\Delta T/T_0$ signal follows closely the S_{11} excitonic band. This confirms that both Z-scan and degenerate pump-probe characterize the same band filling effects. Therefore, the sign of the transient absorption for the degenerate pump-probe experiment, i.e. PA or PB response, directly corresponds to saturable absorption or reverse saturable absorption in the Z-scan measurement. Second, from Fig. 5(c) the sample is found to exhibit a greatly reduced time constant ($\sim 0.3 \text{ ps}$) at 1200 nm as compared to the just-resonant wavelength at 1800 nm ($\sim 1.3 \text{ ps}$). The reduction of recovery time is most probably due to the increasing contribution from S_{22} excitations, where quicker intersubband transitions from S_{22} to S_{11} dominate the relaxation processes.³² The relatively slow recovery time at 2400 nm indicates that semiconducting tubes are primarily accounting for the photocarrier relaxation processes, similar to previous results.^{30,33} Significantly, an unexpected PB to PA transition is seen at $\sim 2100 \text{ nm}$, clearly within the S_{11} band. To confirm such a transition is intrinsic to SWNTs, a non-degenerate pump-probe measurement with higher spectral resolution is performed from 1600 nm to 2400 nm on a SWNT film without polymer matrix. Again, a PB to PA transition is found to occur at $\sim 2100 \text{ nm}$ (See Figure S3 and S4). We assign the onset of the PA band at $\sim 2100 \text{ nm}$ to photoinduced broadening of the S_{11} transition, where carrier effects lead to enhanced oscillator strength for the non-resonant wavelengths.^{34,35} Such a spectral signature suggests that physical effects other than Pauli blocking may play a role in determining the nonlinear absorption of SWNTs.

Conclusions

In summary, by combining single-color Z-scan and de-generate pump-probe spectroscopy over 600-2400 nm, we have for the first time revealed the characteristics of ultrafast nonlinear photoexcitations of SWNT ensembles. The correlation between the Z-scan and pump-probe results allows us to assign features of the nonlinear response to different constituent tubes. We establish multiple insights about the intrinsic optical nonlinearities of SWNTs. Specifically, our results suggest that SWNTs may exhibit ultrafast saturable absorption in a much broader spectral range than previously expected, extending from the visible to the near-infrared. In addition, the wavelength-dependent transient absorption reveals a cut-off for saturable absorption within the semiconducting S₁₁ band, highlighting the role effects other than Pauli blocking may play in the broadband nonlinear absorption in SWNTs. We believe our findings provide a clear interpretation of the broadband ultrafast photoresponse of SWNTs and may have important implications in the design of nanotube based nonlinear optical devices.

Conflict of Interest

The authors declare no competing financial interest.

Acknowledgement

This work is supported by the National Key Basic Research Program of China (2014CB921101), the National Natural Science Foundation of China (61378025,61450110087,61427812,51522201,11474006), Jiangsu Province Shuangchuang Team program, and State Key Laboratory of Advanced Optical Communication Systems Networks, China

Associated content

Supplementary materials accompany this paper.

References

- ¹ O'Connell, M. J.; Bachilo, S. M.; Huffman, C. B.; Moore, V. C.; Strano, M. S.; Haroz, E. H.; Rialon, K. L.; Boul, P. J.; Noon, W. H.; Kittrell, C.; *et al.* Band Gap Fluorescence from Individual Single-Walled Carbon Nanotubes. *Science* **2002**, *297*, 593–596.
- ² Wang, F.; Dukovic, G.; Brus, L. E.; Heinz, T. F. The Optical Resonances in Carbon Nanotubes Arise from Excitons. *Science (80-.)*. **2005**, *308*, 838–841.
- ³ Maeda, a.; Matsumoto, S.; Kishida, H.; Takenobu, T.; Iwasa, Y.; Shiraishi, M.; Ata, M.; Okamoto, H. Large Optical Nonlinearity of Semiconducting Single-Walled Carbon Nanotubes under Resonant Excitations. *Phys. Rev. Lett.* **2005**, *94*, 047404.
- ⁴ Avouris, P.; Freitag, M.; Perebeinos, V. Carbon-Nanotube Photonics and Optoelectronics. *Nat. Photonics* **2008**, *2*, 341–350.
- ⁵ Itkis, M. E.; Borondics, F.; Yu, A.; Haddon, R. C. Bolometric Infrared Photoresponse of Suspended Single-Walled Carbon Nanotube Films. *Science (80-.)*. **2006**, *312*, 413–416.
- ⁶ Liu, Y.; Wang, F.; Wang, X.; Wang, X.; Flahaut, E.; Liu, X.; Li, Y.; Wang, X.; Xu, Y.; Shi, Y.; *et al.* Planar Carbon Nanotube-Graphene Hybrid Films for High-Performance Broadband Photodetectors. *Nat Commun* **2015**, *6*.
- ⁷ Shimamoto, D.; Sakurai, T.; Itoh, M.; Kim, Y. A.; Hayashi, T.; Endo, M.; Terrones, M. Nonlinear Optical Absorption and Reflection of Single Wall Carbon Nanotube Thin Films by Z-Scan Technique. *Appl. Phys. Lett.* **2008**, *92*, 81902.
- ⁸ Chen, Y.-C.; Raravikar, N. R.; Schadler, L. S.; Ajayan, P. M.; Zhao, Y.-P.; Lu, T.-M.; Wang, G.-C.; Zhang, X.-C. Ultrafast Optical Switching Properties of Single-Wall Carbon Nanotube Polymer Composites at 1.55 μm . *Appl. Phys. Lett.* **2002**, *81*, 975.
- ⁹ Liu, K.; Hong, X.; Choi, S.; Jin, C.; Capaz, R. B.; Kim, J.; Wang, W.; Bai, X.; Louie, S. G.; Wang, E.; *et al.* Systematic Determination of Absolute Absorption Cross-Section of Individual Carbon Nanotubes. *Proc. Natl. Acad. Sci. U. S. A.* **2014**, *111*, 7564–7569.
- ¹⁰ Liu, K.; Deslippe, J.; Xiao, F.; Capaz, R. B.; Hong, X.; Aloni, S.; Zettl, A.; Wang, W.; Bai, X.; Louie, S. G.; *et al.* An Atlas of Carbon Nanotube Optical Transitions. *Nat. Nanotechnol.* **2012**, *7*, 325–329.
- ¹¹ Hertel, T.; Moos, G. Electron-Phonon Interaction in Single-Wall Carbon Nanotubes: A Time-Domain Study. *Phys. Rev. Lett.* **2000**, *84*, 5002–5005.

-
- ¹² Ostojic, G. N.; Zaric, S.; Kono, J.; Strano, M. S.; Moore, V. C.; Hauge, R. H.; Smalley, R. E. Interband Recombination Dynamics in Resonantly Excited Single-Walled Carbon Nanotubes. *Phys. Rev. Lett.* **2004**, *92*, 117402–1.
- ¹³ Ostojic, G. N.; Zaric, S.; Kono, J.; Moore, V. C.; Hauge, R. H.; Smalley, R. E. Stability of High-Density One-Dimensional Excitons in Carbon Nanotubes under High Laser Excitation. *Phys. Rev. Lett.* **2005**, *94*, 2–5.
- ¹⁴ Korovyanko, O. J.; Sheng, C.-X. C.-X.; Vardeny, Z. V.; Dalton, A. B.; Baughman, R. H. Ultrafast Spectroscopy of Excitons in Single-Walled Carbon Nanotubes. *Phys. Rev. Lett.* **2004**, *92*, 017403.
- ¹⁵ Lüer, L.; Lanzani, G.; Crochet, J.; Hertel, T.; Holt, J.; Vardeny, Z. V. Ultrafast Dynamics in Metallic and Semiconducting Carbon Nanotubes. *Phys. Rev. B - Condens. Matter Mater. Phys.* **2009**, *80*, 4–8.
- ¹⁶ Ichida, M.; Hamanaka, Y.; Kataura, H.; Achiba, Y.; Nakamura, a. Ultrafast Relaxation Dynamics of Photoexcited States in Semiconducting Single-Walled Carbon Nanotubes. *Phys. B Condens. Matter* **2002**, *323*, 237–238.
- ¹⁷ Set, S. Y.; Yaguchi, H.; Tanaka, Y.; Jablonski, M. Ultrafast Fiber Pulsed Lasers Incorporating Carbon Nanotubes. *IEEE J. Sel. Top. Quantum Electron. Electron.* **2004**, *10*, 137–146.
- ¹⁸ Sakakibara, Y.; Tatsuura, S.; Kataura, H.; Tokumoto, M.; Achiba, Y. Near-Infrared Saturable Absorption of Single-Wall Carbon Nanotubes Prepared by Laser Ablation Method. *Jpn. J. Appl. Phys.* **2003**, *42*, L494–L496.
- ¹⁹ Wang, F.; Rozhin, A. G.; Scardaci, V.; Sun, Z.; Hennrich, F.; White, I. H.; Milne, W. I.; Ferrari, A. C. Wideband-Tuneable, Nanotube Mode-Locked, Fibre Laser. *Nat. Nanotechnol.* **2008**, *3*, 738–742.
- ²⁰ Wang, F.; Rozhin, A. G.; Scardaci, V.; Sun, Z.; Hennrich, F.; White, I. H.; Milne, W. I.; Ferrari, A. C. Wideband-Tuneable, Nanotube Mode-Locked, Fibre Laser. *Nat. Nanotechnol.* **2008**, *3*, 738–742.
- ²¹ Hasan, T.; Sun, Z.; Wang, F.; Bonaccorso, F.; Tan, P. H.; Rozhin, A. G.; Ferrari, A. C. Nanotube–Polymer Composites for Ultrafast Photonics. *Adv. Mater.* **2009**, *21*, 3874–3899.
- ²² Wang, F.; Rozhin, A. G.; Sun, Z.; Scardaci, V.; White, I. H.; Ferrari, A. C. Soliton Fiber Laser Mode-Locked by a Single-Wall Carbon Nanotube-Polymer Composite Film. *Phys. status solidi* **2008**, *245*, 2319–2322.

-
- ²³ (1) Kivistö, S.; Hakulinen, T.; Kaskela, A.; Aitchison, B.; Brown, D. P.; Nasibulin, A. G.; Kauppinen, E. I.; Härkönen, A.; Okhotnikov, O. G. Carbon Nanotube Films for Ultrafast Broadband Technology. *Opt. Express* **2009**, *17*, 2358–2363.
- ²⁴ Hasan, T.; Sun, Z.; Tan, P.; Popa, D.; Flahaut, E.; Kelleher, E. J. R.; Bonaccorso, F.; Wang, F.; Jiang, Z.; Torrisi, F.; *et al.* Double-Wall Carbon Nanotubes for Wide-Band, Ultrafast Pulse Generation. *ACS Nano* **2014**, *8*, 4836–4847.
- ²⁵ Tolstik, N.; Okhotnikov, O.; Sorokin, E.; Sorokina, I. T. Femtosecond Cr:ZnS Laser at 2.35 μm Mode-Locked by Carbon Nanotubes. *Proc. SPIE*, 2014, *8959*, 89591A – 89591A – 6.
- ²⁶ N, K.; Kumar, S.; Sood, A. K.; Guha, S.; Krishnamurthy, S.; Rao, C. N. R. Large Nonlinear Absorption and Refraction Coefficients of Carbon Nanotubes Estimated from Femtosecond Z-Scan Measurements. *Appl. Phys. Lett.* **2007**, *91*, 10.
- ²⁷ Strano, M. S.; Doorn, S. K.; Haroz, E. H.; Kittrell, C.; Hauge, R. H.; Smalley, R. E. Assignment of (n, M) Raman and Optical Features of Metallic Single-Walled Carbon Nanotubes. *Nano Lett.* **2003**, *3*, 1091–1096.
- ²⁸ Saito, R.; Fujita, M.; Dresselhaus, G.; Dresselhaus, M. S. Electronic Structure of Chiral Graphene Tubules. *Appl. Phys. Lett.* **1992**, *60*, 2204–2206.
- ²⁹ Agrawal, G. P. Applications of Nonlinear Fiber Optics,” (Academic Press, San Diego, 2001)
- ³⁰ Lauret, J.-S.; Voisin, C.; Cassabois, G.; Delalande, C.; Roussignol, P.; Jost, O.; Capes, L. Ultrafast Carrier Dynamics in Single-Wall Carbon Nanotubes. *Phys. Rev. Lett.* **2003**, *90*, 057404.
- ³¹ Li, X.; Wang, Y.; Wang, Y.; Zhao, W.; Yu, X.; Sun, Z.; Cheng, X.; Yu, X.; Zhang, Y.; Wang, Q. J. Nonlinear Absorption of SWNT Film and Its Effects to the Operation State of Pulsed Fiber Laser. *Opt. Express* **2014**, *22*, 17227–17235.
- ³² Manzoni, C.; Gambetta, A.; Menna, E.; Meneghetti, M.; Lanzani, G.; Cerullo, G. Intersubband Exciton Relaxation Dynamics in Single-Walled Carbon Nanotubes. *Phys. Rev. Lett.* **2005**, *94*, 207401.
- ³³ Huang, L.; Pedrosa, H. N.; Krauss, T. D. Ultrafast Ground-State Recovery of Single-Walled Carbon Nanotubes. *Phys. Rev. Lett.* **2004**, *93*, 017403.
- ³⁴ Jung, Y.; Slipchenko, M. N.; Liu, C. H.; Ribbe, A. E.; Zhong, Z.; Yang, C.; Cheng, J. X. Fast Detection of the Metallic State of Individual Single-Walled Carbon Nanotubes Using a Transient-Absorption Optical Microscope. *Phys. Rev. Lett.* **2010**, *105*, 1–4.

³⁵ Liu, K.; Hong, X.; Zhou, Q.; Jin, C.; Li, J.; Zhou, W.; Liu, J.; Wang, E.; Zettl, A.; Wang, F. High-Throughput Optical Imaging and Spectroscopy of Individual Carbon Nanotubes in Devices. *Nat. Nanotechnol.* **2013**, *8*, 917–922.

Figures

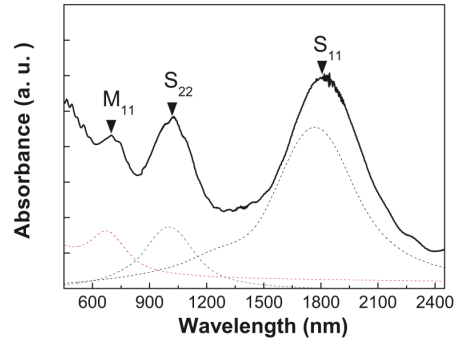


Figure 1. Measured UV-vis-IR absorption curve of the SWNTs. Dash lines indicate calculated absorption for S11 (black), S22 (blue) and M11 (red) transitions.

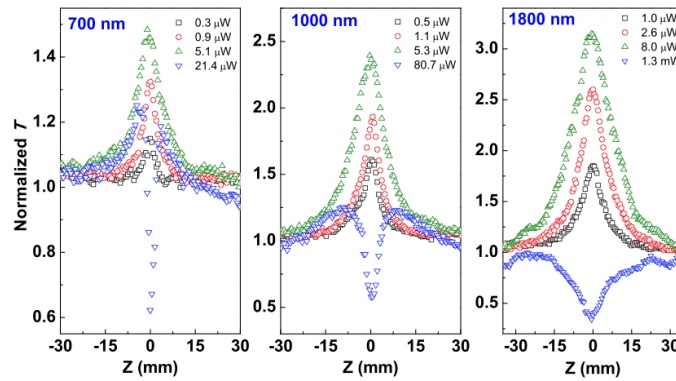


Figure 2. Open-aperture Z-scan results for on-resonance wave-lengths: 700 nm (M₁₁), 1000 nm (S₂₂), 1800 nm (S₁₁).

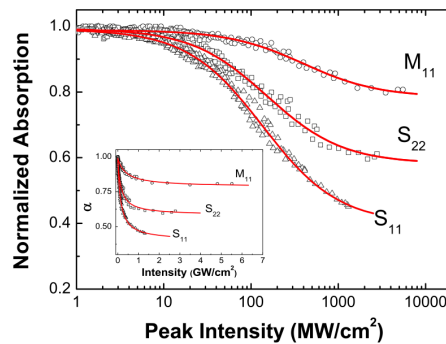


Figure 3. Normalized absorption for 700 nm (M₁₁), 1000 nm (S₂₂), 1800 nm (S₁₁), with best saturable absorption fittings (red solid lines).

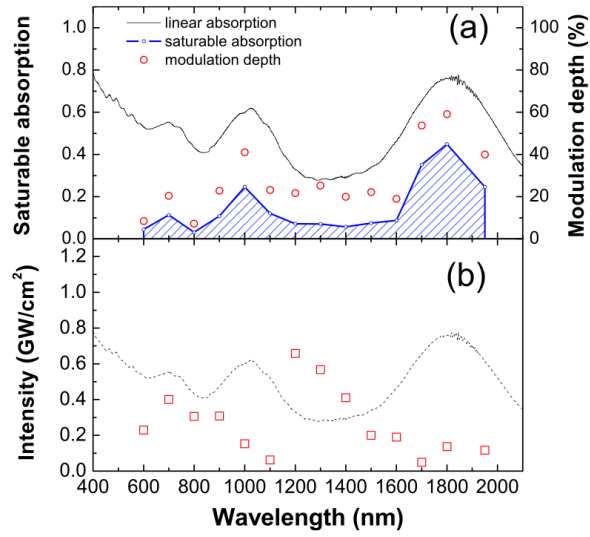


Figure 4. (a) Measured modulation depth from 600 nm to 1950 nm (the shaded area corresponds to saturable absorption); (b) Measured saturation intensity in the same wavelength range.

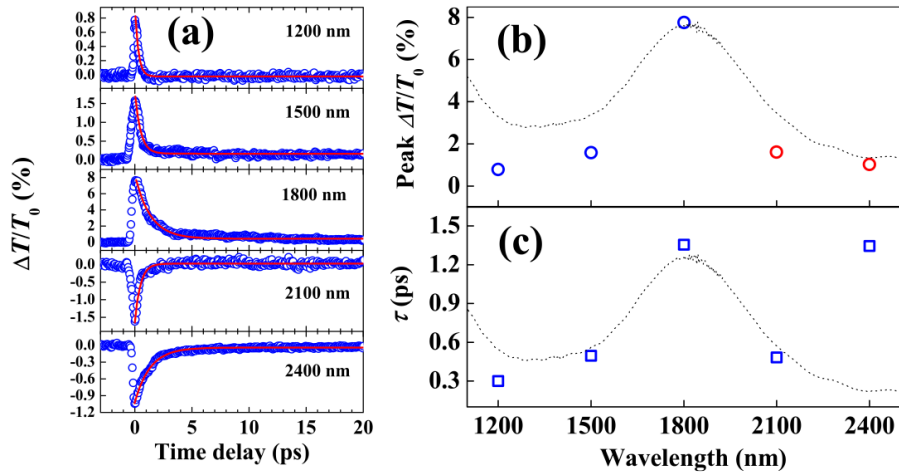


Figure 5. (a) Transient transmission for 1200, 1500, 1800, 2100 and 2400 nm excitation wavelengths; (b) Peak $\Delta T/T_0$ and (c) relaxation times as a function of excitation wavelengths.